Prepublished copy

Nature Environment & Pollution Technology

This is a peer-reviewed prepublished version of the paper to be published in Vol. 25, No. 2, June 2026 issue

Original Research

Tailored Nitrogen Sites on Biomass-Derived Activated Carbon for Enhanced Formaldehyde Detection at Room Temperature

Thanattha Chobsilp[1], Alongkot Treetong[2], Visittapong Yordsri[3], Saowaluk Inpaeng[4], Jaruvit Sukkasem[5], Winadda Wongwiriyapan[6] and Worawut Muangrat[1]†

[1]Department of Advanced Materials Engineering, Faculty of Engineering, Burapha University, Chonburi, 20131, Thailand

[2]National Nanotechnology Center, Pathumthani 12120, Thailand

[3]National Metal and Materials Technology Center, Pathumthani 12120, Thailand

[4]Pattaya Center Administration Division, Thammasat University Pattaya Campus, Chonburi 20150, Thailand

[5]Filter Match Co., Ltd., Bangkok 10520, Thailand

[6]College of Materials Innovation and Technology, King Mongkut's Institute of Technology Ladkrabang, Bangkok 10520, Thailand

†Corresponding author: Worawut Muangrat; worawut.mu@buu.ac.th

Key Words	Nitrogen-doped activated carbon, Formaldehyde, Ammonia heat treatment, Gas sensors, Sustainable development goal
DOI	https://doi.org/10.46488/NEPT.2026.v25i02.D1842 (DOI will be active only after the final publication of the paper)
Citation for the Paper	Chobsilp, T., Treetong, A., Yordsri, V., Inpaeng, S., Sukkasem, J., Wongwiriyapan, W. and Muangrat, W., 2026. Tailored nitrogen sites on biomass-derived activated carbon for enhanced formaldehyde detection at room temperature. *Nature Environment and Pollution Technology*, 25(2), D1842. https://doi.org/10.46488/NEPT.2026.v25i02.D1842

ABSTRACT

This research introduces nitrogen atom into biomass-derived activated (AC) to enhance their sensitivity to formaldehyde vapor at room temperature. Nitrogen-doped activated carbon (N-AC) derived from coconut shells was successfully prepared by heat treatment with ammonia (NH_3) at 800°C. The atomic ratio of nitrogen to carbon in N-AC is approximately 4.1 at%. AC and N-AC were separately mixed with ethanol and then dropped onto printed circuit board with Au/Cu electrodes, serving as the sensor substrate. As-fabricated AC and N-AC sensors were exposed to formaldehyde concentrations ranging from 1 to 100 parts per million (ppm) at room temperature. N-AC sensor demonstrated a sensor response approximately 5- to 6-fold higher than that of the AC sensor. The enhancement of formaldehyde sensitivity is attributed to the increased surface area, porosity and nitrogen doping into AC. The sensing mechanism can be explained by charge transfer from formaldehyde molecules to sensing materials. Nitrogen-doped sites play a crucial role in improving formaldehyde adsorption due to their high binding energy and significant charge transfer, resulting in an enhanced sensor response. This work proposes an effective method involving NH_3 heat treatment for biomass-derived AC to improve surface area, porosity, and nitrogen doping of AC to enhance the sensitivity of formaldehyde detection at room temperature.

INTRODUCTION

Air pollution caused by volatile organic compounds (VOCs), is a serious concern due to its harmful effects on human health and the environment. VOCs can lead to health problems such as lung inflammation, respiratory damage, cancer, and death at high levels (Ogbodo et al. 2022, Shen et al. 2024). The control of air quality is a necessary and urgent issue. High-performance liquid chromatography and gas chromatography-mass spectrometry are excellent conventional methods for analyzing VOCs, with high sensitivity, selectivity, and reliability (Reinnig et al. 2008, Delgado-Rodríguez et al. 2012, Xu et al. 2023). Nevertheless, the drawbacks of high-performance liquid chromatography and gas chromatography-mass spectrometry include high cost, complex procedures, time consumption, lack of real-time monitoring, and requiring expert technicians to operate equipment. Recently, gas sensor technology has played a crucial role in monitoring air pollution. The advantages of gas sensors is a simple operation, low cost, fast response time, portability and real-time monitoring. Activated carbon (AC) is a porous material with high specific surface area, porosity, well-defined pore size distribution and chemical stability (Xue et al. 2019), which is suitable for application as sensing materials in gas sensor technology. To achieve the sustainable development goals (SDGs), the production of AC from agricultural waste has attracted considerable attention (Chew et al. 2023, Neme et al. 2022, Ukanwa et al. 2019). Using agricultural waste to produce AC supports waste reduction and resource efficiency, which promotes responsible consumption and production (SDG 12). A gas sensor based on biomass-derived AC for detecting VOCs such as acetone, ethanol, methanol vapors, and ammonia gas was proposed (Ranasinghe et al. 2024). Sensor-based on AC shows the response to ammonia gas and VOCs, particularly methanol vapor. To enhance the sensing performance, biomass-derived AC has been combined with metal oxides and polymers for the detection of ammonia (NH_3) (Travlou et al. 2017), hydrogen sulfide (Bibi et al. 2023, Luo et al. 2023, Rodiawan et al. 2024), acetone, and ethanol (Chao et al. 2019, Jena et al. 2022). Although AC combined with metal oxides or polymers significantly improves sensing performance, AC-metal oxide-based gas sensors require high-temperature operation and consume high power to achieve high performances, whereas AC-polymer-based sensors suffer from poor thermal stability, limited selectivity, and degradation. Heteroatom doping, such as nitrogen atom, into the surface of biomass-derived AC, is another approach to enhance the adsorption of NH_3 molecules (Travlou et al. 2015, Travlou et al. 2016, Kyokunzire et al. 2024). Nitrogen atoms were incorporated into biomass-derived AC through nitric acid soaking and melamine heat treatment. It can be found that nitrogen sites play an important role in NH_3 adsorption. So far, biomass-derived AC, combined with metal oxides, polymers, and heteroatom doping have been widely used for the detection of a few gases and vapors, such as NH_3, hydrogen sulfide, acetone, ethanol, and methanol.

Formaldehyde is one of the toxic VOCs that is released from various sources such as building materials, furniture, tobacco smoke, and combustion processes. Formaldehyde can irritate of skin, eyes, nose, and throat, inflammation bronchi and lungs, nasal cavity cancer, and leukemia (Golden 2011, Kim et al. 2011). The National Institute for Occupational Safety and Health (NIOSH) defines the immediately dangerous to life or health

(IDLH) concentration for formaldehyde as 20 parts per million (ppm), and the permissible short-term exposure limit (STEL) as 2 ppm in air over 15 min (Huang et al. 2024). Therefore, monitor and early warning for formaldehyde exposure are essential to ensure the occupational safety. In this work, formaldehyde sensors were fabricated using AC and nitrogen-doped AC (N-AC) as the sensing materials. Coconut shells were used as the biomass source for producing AC. N-AC was prepared by heat treatment under an NH_3 atmosphere. N-AC sensor exhibited remarkably improved formaldehyde detection at room temperature compared to the undoped AC.

2. MATERIALS AND METHODS

2.1. Preparation of Nitrogen-Doped Activated Carbon

Coconut shell-derived AC (VPAC-P4/1050)-supported FILTER MATCH Co., Ltd. (Thailand) was placed into a horizontal tube furnace under argon gas with a flow rate of 500 mL/min. The temperature was raised from room temperature to 800°C at a rate of 5°C/min. AC was treated at 800°C under a mixture of argon (100 mL/min) and ammonia (50 mL/min) gases for 60 min. Finally, as-doped samples were cooled to room temperature under argon gas (500 mL/min). Both AC and N-AC were ground into a fine powder.

2.2. Characterization Techniques

The morphologies were characterized by scanning electron microscopy (SEM, JEOL, JSM-7800F). The crystallinity was analyzed by Raman spectroscopy (Horiba LabRam HR) using an Ar laser light source with a wavelength of 532 nm. X-ray photoelectron spectroscopy (XPS, AXIS Ul-traDLD, Kratos Analytical) was utilized to analyze the surface elements and chemical states. Surface area and porosity were characterized by the Brunauer-Emmett-Teller (BET, Micromeritics, TriStarII 3020) from the nitrogen adsorption-desorption isotherms at 77 K.

2.3. Gas Sensor Fabrication and Measurement

10 mg of AC and N-AC were separately dispersed in 10 µL of ethanol using ultrasonication for 60 min. A 50 µL of the mixed sample-ethanol solution was dropped onto the printed circuit board in 30 drops while maintaining the sensor substrate at 80°C during the drop-casting process. To evaporate the residual solvent in the sensing materials, as-fabricated AC and N-AC sensors were kept in an oven at 80°C for 60 min. The percent of the sensor response (SR%) was recorded as the change in the electrical resistance under air and formaldehyde atmospheres using a multimeter (UNI-T; UT71D). The SR% can be calculated using Equation (1), whereas R_{HCHO} and R_{air} are the electrical resistance of the sensor under formaldehyde vapor and air atmosphere, respectively. As-fabricated AC and N-AC sensors were separately placed in a stainless-steel chamber and kept under an air atmosphere for 10 min to provide the baseline signal of the sensors. The formaldehyde was injected into the detection system and kept in the closed system for 10 min to observe the change in electrical resistance

under formaldehyde exposure. Then, all sensors were recovered in an air atmosphere for 10 min. The concentration of formaldehyde varied in the range of 1–100 ppm.

$$SR\% = ((R_{HCHO} - R_{air})/R_{air}) \times 100 \quad \ldots(1)$$

3. RESULTS OR RESULTS AND DISCUSSIONS

3.1. Characterization Results

The surface morphologies AC and N-AC were characterized by SEM. SEM images revealed that both AC and N-AC consist of irregularly shaped micron-sized carbon particles, as shown in Fig. 1(a,c). At high magnification SEM images showed that AC and N-AC exhibit porous morphologies, as shown in Fig. 1(b,d). Furthermore, the pore structure in N-AC increased after NH_3 heat treatment. To confirm the effect of NH_3 heat treatment on the increase in surface area and porosity, AC and N-AC were evaluated using BET analysis, as discussed later.

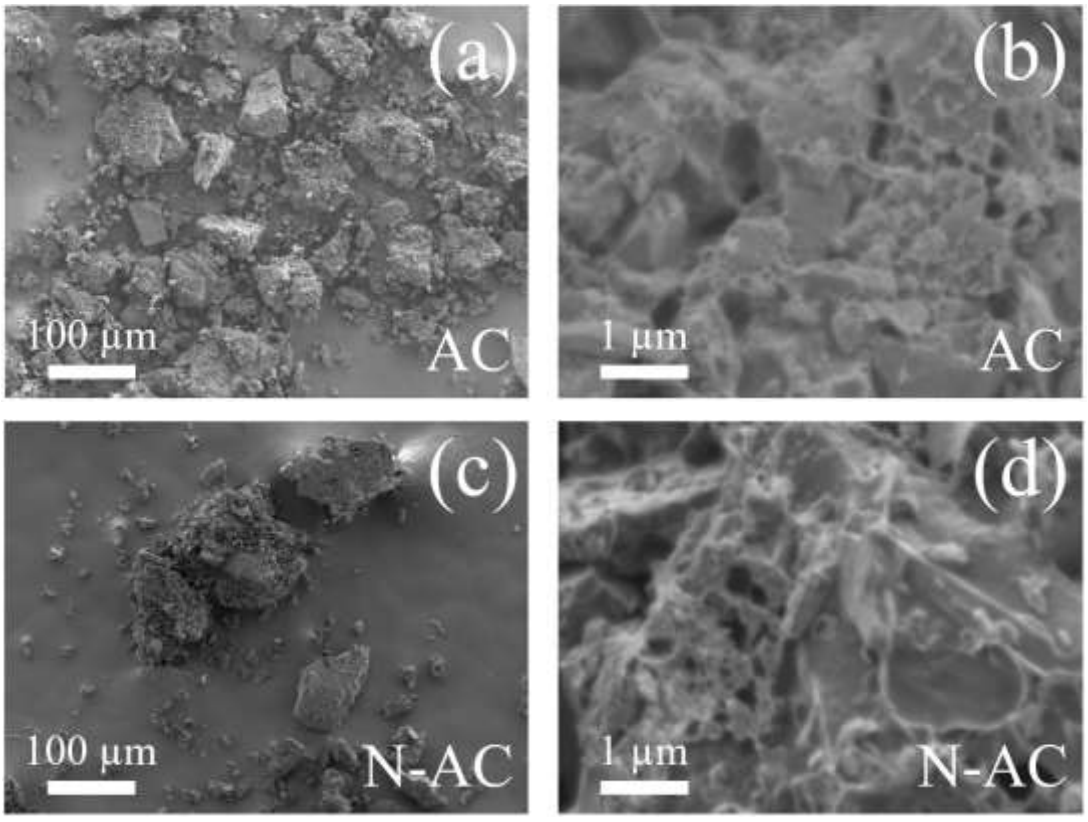

Fig. 1: Low- and high-magnification SEM images of (a,b) AC and (c,d) N-AC.

Raman spectra of AC and N-AC are shown in Fig. 2(a). Both AC and N-AC exhibit two peaks at ~1340 and ~1590 cm^{-1}, corresponding to the disordered graphitic (D-band) and crystalline graphitic (G-band) structures, respectively (Liu et al. 2017, Shimodaira et al. 2002). The ratio value of the D-band to the G-band (I_D/I_G) can be used to estimate the degree of crystallinity. Namely, a high I_D/I_G value indicates low crystallinity (Liu

et al. 2017, Shimodaira et al. 2002). The I_D/I_G ratios of AC and N-AC were 1.06±0.04 and 1.17±0.02, respectively. The increase in the I_D/I_G ratio implied a decrease in crystallinity. The decrease in crystallinity is attributed to the incorporation of nitrogen atoms into graphitic structure (Qian et al. 2019). Fig. 2(b) presents the N_2 adsorption–desorption isotherms at 77 K for AC and N-AC, obtained from BET analysis. The N_2 adsorption isotherms exhibit characteristics of both type I and IV isotherms, according to the International Union of Pure and Applied Chemistry classification. The isotherms are typical of microporous materials (Kumar et al. 2016, Zhang et al. 2018). After NH_3 heat treatment, the total specific surface area, total pore volume, micropore volume, and pore diameter increased, as shown in Table1. The total surface areas of AC and N-AC were 749.19 and 822.11 $m^2.g^{-1}$, respectively, while the total pore volumes were 0.3213 and 0.3515 $cm^3.g^{-1}$, respectively. The micropore volumes of AC and N-AC were 0.2903 and 0.3158 $cm^3.g^{-1}$, respectively, while their pore diameters were 1.5404 and 1.5442 nm, respectively. NH_3 heat treatment not only induces the incorporation of nitrogen atoms into the AC structure but also increases the surface area and porosity due to the etching effect of NH_3 (Katsura et al. 1998, Mochizuki et al. 2022).

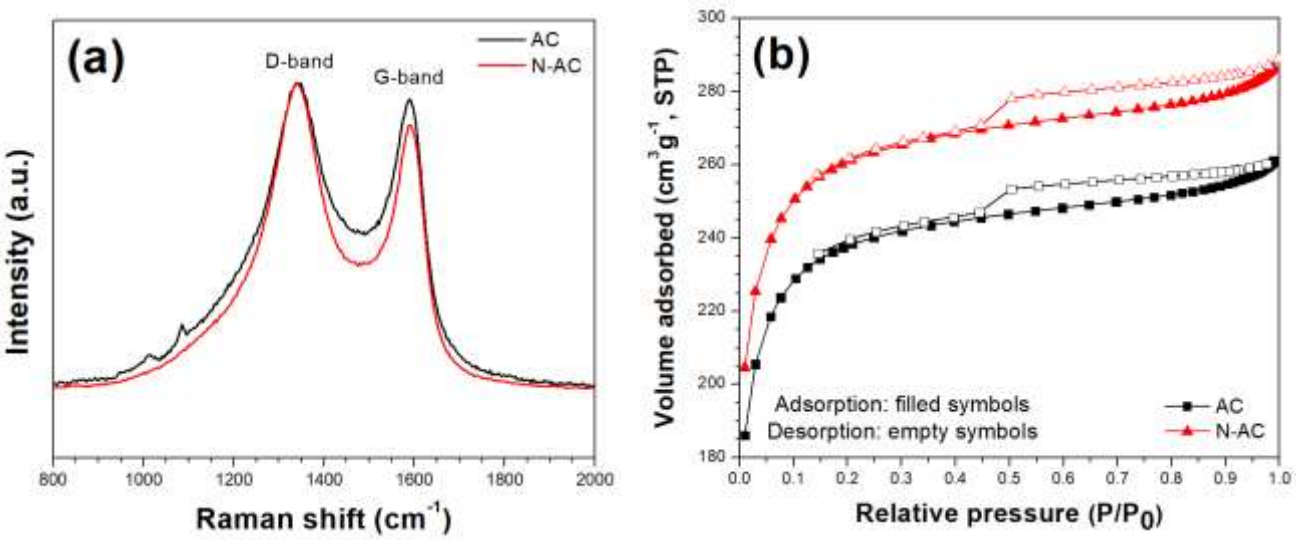

Fig. 2: (a) Raman spectra of AC and N-AC. (b) Nitrogen adsorption-desorption isotherms of AC and N-AC.

Table 1: The total surface area, total pore volume, micropore volume, and pore diameter of AC and N-AC.

Sample	Total surface area ($m^2.g^{-1}$)	Total pore volume ($cm^3.g^{-1}$)	$V_{micropore}$ ($cm^3.g^{-1}$)	Pore diameter (nm)
AC	749.19	0.3213	0.2903	1.5404
N-AC	822.11	0.3515	0.3158	1.5442

The chemical state and composition were analyzed by XPS. As shown in the survey spectra in Fig. 3(a), Ac and N-AC exhibited two prominent peaks at ~285 and ~532 eV, which correspond to the C1s and O1s peaks, respectively (Lennon et al. 2002, Ojha et al. 2025). Additionally, the N1s peak was observed at ~400 eV in the N-AC, confirming the successful incorporation of nitrogen atoms into the carbon structure. The C1s

spectra of AC and N-AC were deconvoluted to the C–C, C–O, C=O, and O–C=O, as shown in Fig. 3(b). Fig. 3(c) presents the O1s spectra of AC and N-AC, which consist of contributions from C=O, C–O, O–C=O, and O–H (Chen et al. 2020, Jerng et al. 2011, Zhang et al. 2018). Fig. 3(d) shows the N1s spectra of AC and N-AC, which exhibit three deconvoluted bonding configurations: pyridinic-N, pyrrolic-N, and graphitic-N (He et al. 2022, Sun et al. 2019). The atomic ratio of nitrogen to carbon in N-AC is 4.81 at.%. The contents of pyridinic-N, pyrrolic-N, and graphitic-N in N-AC were 2.56, 1.48, and 0.77 at.%, respectively.

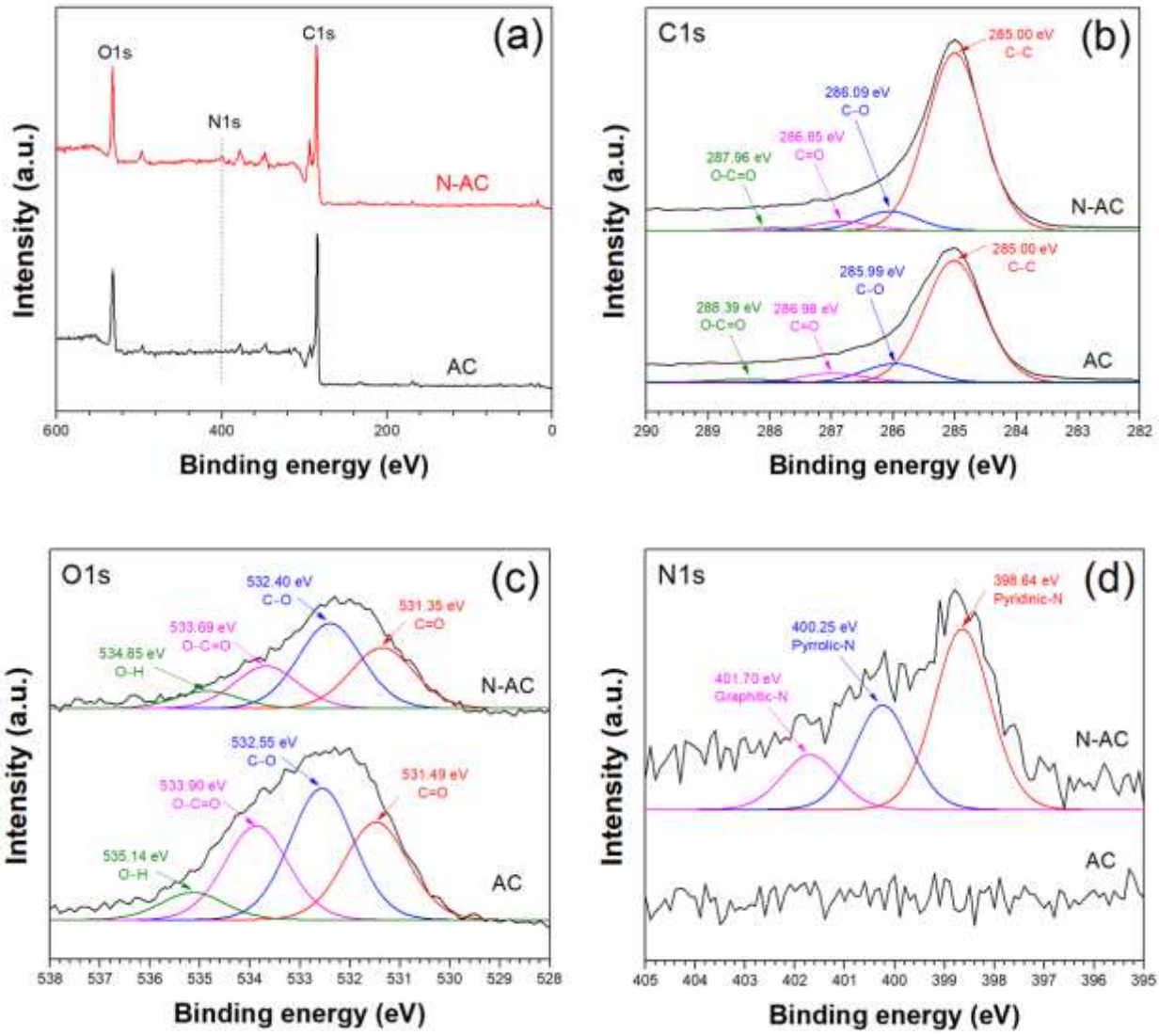

Fig. 3: (a) Survey spectra of AC and N-AC. (b) C1s, (c) O1s and (d) N1s spectra of AC and N-AC.

3.2. Gas Sensor Results

Fig. 4(a-c) illustrates the time-dependent response of as-fabricated AC and N-AC sensors to formaldehyde in the concentration range of 10-100 ppm at room temperature. The electrical resistance of as-fabricated AC and N-AC sensors increases upon exposure to formaldehyde vapor and recovers to its initial electrical resistance under air exposure. N-AC sensor was unable to recover to its initial electrical resistance under air ambient. The

reversibility of the sensor can be improved by UV irradiation and heating. The sensor responses (%) of the as-fabricated AC sensors were 3.22, 3.57, and 4.34% at formaldehyde concentrations of 10, 50, and 100 ppm, respectively, while the responses of the as-fabricated N-AC sensors were 7.54, 15.79, 20.68, and 26.72 at 1, 10, 50, and 100 ppm, respectively. The sensing results demonstrated that the N-AC sensor exhibited 4.90-, 5.79-, and 6.16-fold higher responses than that of the AC sensor at formaldehyde concentrations of 10, 50, and 100 ppm, respectively. The formaldehyde-sensing mechanism is attributed to the charge transfer between formaldehyde molecule and sensing materials. Upon adsorption, formaldehyde molecules donate electron to sensing materials, leading to a decrease in their electrical resistance (Kyokunzire et al. 2024, Ranasinghe et al. 2024, Travlou, et al. 2015). In the case of N-AC, according to theoretical and experimental studies (Chobsilp et al. 2022, Dwivedi et al. 2020, Prakash et al. 2022) have demonstrated that nitrogen sites play a crucial role in enhancing the interaction between N-AC and formaldehyde molecules through chemisorption, owing to their high binding energy, resulting in a significantly enhanced sensor response. The strong interaction hinders the desorption formaldehyde molecules from the N-AC surface, as evidenced by the slow recovery of as-fabricated sensor to their initial electrical resistance. Additionally, in terms of specific surface area and volume of micropore, N-AC exhibits 9.73% and 8.78% higher values, respectively, compared to undoped AC. The enhancement of formaldehyde detection is also attributed the increased surface area. Micropores in porous carbon materials play an important role in gas adsorption (Bai et al. 2016, Do et al. 2015). Thus, a high surface area and micropore volume provide more adsorption sites for formaldehyde molecules. Fig.4(d) presents the time-dependent response of N-AC sensors exposed to formaldehyde at 1-100 ppm. The results indicated that the sensor response increases with higher formaldehyde concentrations due to a large amount of formaldehyde molecules adsorption on the surface of N-AC, resulting in a higher in sensor response.

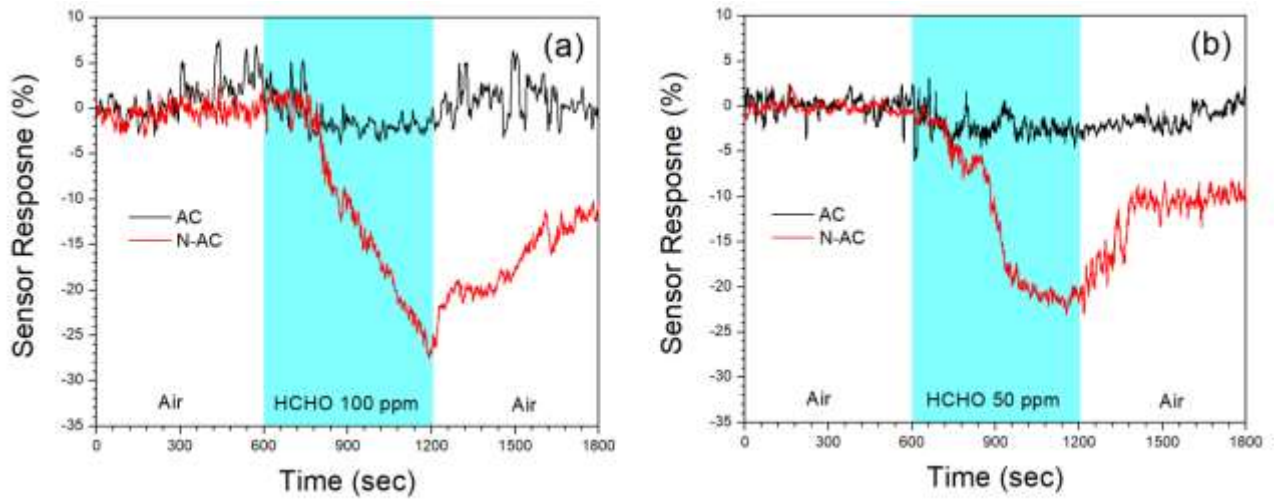

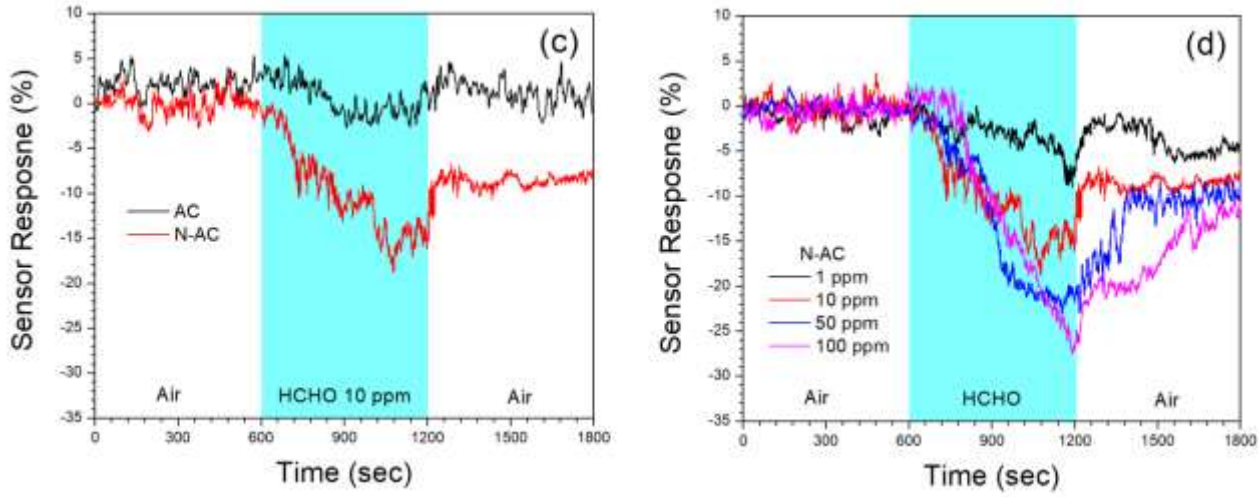

Fig. 4: (a) Time-dependent sensor response of AC and N-AC sensors exposed to the formaldehyde concentrations of (a) 100, (b) 50, and (c) 10 ppm at room temperature. (d) Time-dependent sensor response of N-AC sensor exposed to formaldehyde at 1-100 ppm at room temperature.

Fig. 5 illustrates the sensor responses of AC and N-AC sensors as a function of formaldehyde concentration. For the AC sensor, the relationship between sensor response and formaldehyde displays a linear response in the range of 10-100 ppm. In the case of the N-AC sensor, the sensor response increases rapidly with increasing formaldehyde concentration from 1 to 50 ppm. The sensor response of the N-AC sensor ap-pears to saturate at formaldehyde concentrations higher than 100 ppm. The N-AC sensor can detect formaldehyde concentrations as low as 1 ppm, which is lower than the standard IDLH level of 20 ppm and the STEL of 1 ppm, as specified by NIOSH. This work demonstrated that the N-AC sensor exhibits high sensitivity for formaldehyde detection at room temperature with a LOD of 1 ppm. To improve the sensor performance, the selectivity of N-AC toward other VOCs and gases and long-term stability will be investigated in the future work.

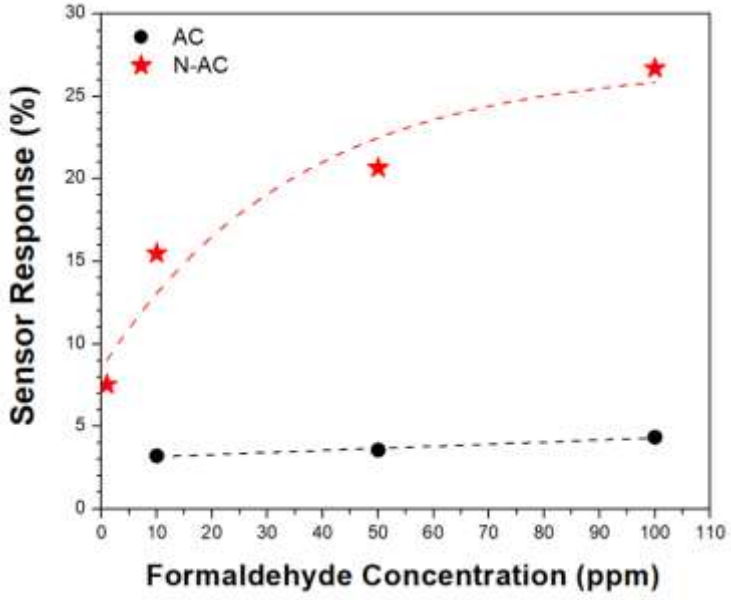

Fig. 4: Sensor responses of AC and N-AC sensors as a function of formaldehyde concentration.

4. CONCLUSIONS

A highly sensitive formaldehyde sensor was successfully developed through the incorporation of nitrogen into the biomass-derived AC structure. NH_3 heat treatment was employed as an effective method to enhance the surface area, porosity, and nitrogen doping into AC structure. As-fabricated N-AC sensor exhibited a 5- to 6-fold enhancement in the response to formaldehyde concentrations ranging from 10 to 100 ppm at room temperature. The enhanced sensitivity is derived from the combination of high surface area, increased porosity, and the presence of nitrogen-doped sites on the AC. The sensing mechanism is attributed to charge transfer between the sensing material and formaldehyde molecules, facilitated by nitrogen sites on the AC surface, which induce strong interactions with formaldehyde. This work demonstrates that surface and porous structure modification via NH_3 heat treatment offers a promising approach for developing practical and high-sensitivity formaldehyde sensing materials operating at room temperature. This work supports the SDG related to Industry, Innovation, and Infrastructure (SDG 9) as well as Responsible Consumption and Production (SDG 12).

Author Contributions: Conceptualization, J.S. and W.M.; methodology, T.C., A.T., V.Y., S.I. and W.M; validation, T.C., A.T., V.Y., S.I. and W.M.; formal analysis, T.C., V.Y. and W.M.; investigation, T.C. and W.M.; writing—original draft preparation, T.C.; writing—review and editing, W.M.; supervision, W.W. and W.M.; project administration, T.C.; funding acquisition, W.M. All authors have read and agreed to the published version of the manuscript.

Funding: This research was funded by Burapha University, grant number SDG 4/2568.

Institutional Review Board Statement: Not applicable.

Informed Consent Statement: Not applicable.

Acknowledgments: We extend our gratitude to FILTER MATCH Co., Ltd. (Thailand) for supporting the coconut shell-derived AC.

Conflicts of Interest: The authors declare no conflicts of interest.

REFERENCES

1. Bai, B.C. and Bae, T.-S., 2016. Pore structure control of activated carbon fiber for CO gas sensor electrode. *Carbon Letters*, 18, pp.76–79. [https://doi.org/10.5714/CL.2016.18.076]
2. Bibi, A., Santiago, K.S., Yeh, J.M. and Chen, H.H., 2023. Valorization of agricultural waste as a chemiresistor H_2S-gas sensor: A composite of biodegradable-electroactive polyurethane-urea and activated-carbon composite derived from coconut-shell waste. *Polymers*, 15(3), pp.685. [https://doi.org/10.3390/polym15030685]
3. Chao, J., Chen, Y., Xing, S., Zhang, D. and Shen, W., 2019. Facile fabrication of ZnO/C nanoporous fibers and ZnO hollow spheres for high-performance gas sensor. *Sensors and Actuators B: Chemical*, 298, pp.126927. [https://doi.org/10.1016/j.snb.2019.126927]

4. Chen, X., Wang, X. and Fang, D., 2020. A review on C1s XPS spectra for some kinds of carbon materials. *Fullerene, Nanotubes and Carbon Nanostructures*, 28(12), pp.1048–1058. [https://doi.org/10.1080/1536383X.2020.1794851]
5. Chew, T.W., H'Ng, P.S., Teong, B.C., Abdullah, L.C., Chin, K.L., Lee, C.L., Mohd Nor Hafizuddin, B.M.S. and TaungMai, L., 2023. A review of bio-based activated carbon properties produced from different activating chemicals during chemical activation process on biomass and its potential for Malaysia. *Materials*, 16(23), pp.7365. [https://doi.org/10.3390/ma16237365]
6. Chobsilp, T., Threrujirapapong, T., Yordsri, V., Treetong, A., Inpaeng, S., Tedsree, K., Ayala, P., Pichler, T., Shi, L. and Muangrat, W., 2022. Highly sensitive and selective formaldehyde gas sensors based on polyvinylpyrrolidone/nitrogen-doped double-walled carbon nanotubes. *Sensors*, 22(23), p.9329. [https://doi.org/10.3390/s22239329]
7. Do, D.D., Tan, S.L.J., Zeng, Y., Fan, C., Nguyen, V.T., Horikawa, T. and Nicholson, D., 2015. The interplay between molecular layering and clustering in adsorption of gases on graphitized thermal carbon black—spill-over phenomenon and the important role of strong sites. *Journal of Colloid and Interface Science*, 446, pp.98–113. [https://doi.org/10.1016/j.jcis.2015.01.028]
8. Delgado-Rodríguez, M., Ruiz-Montoya, M., Giraldez, I., López, R., Madejón, E. and Díaz, M.J., 2012. Use of electronic nose and GC-MS in detection and monitoring of some VOCs. *Atmospheric Environment*, 51, pp.278–285. [https://doi.org/10.1016/j.atmosenv.2012.01.045]
9. Dwivedi, N. and Shukla, R.K., 2020. Theoretical study of pure/doped (nitrogen and boron) carbon nanotubes for chemical sensing of formaldehyde. *SN Applied Sciences*, 2, p.262. [https://doi.org/10.1007/s42452-020-2055-2]
10. Golden, R., 2011. Identifying an indoor air exposure limit for formaldehyde considering both irritation and cancer hazards. *Critical Reviews in Toxicology*, 41(8), pp.672–721. [https://doi.org/10.3109/10408444.2011.573467]
11. He, S., Chen, Q., Chen, G., Shi, G., Ruan, C., Feng, M. et al., 2022. N-doped activated carbon for high-efficiency ofloxacin adsorption. *Microporous and Mesoporous Materials*, 341, 111848. [https://doi.org/10.1016/j.micromeso.2022.111848]
12. Huang, C.A., Shapiro, L. and Feldman, S.R., 2024. Formalin safety in the outpatient setting. *JAAD Reviews*, 2, pp.140–144. [https://doi.org/10.1016/j.jdrv.2024.10.005]
13. Jena, L., Sarangi, S.N., Soren, D., Deheri, P.K. and Pattojoshi, P., 2022. Facile two-step synthesis of chemiresistive sensor based on γ-Fe_2O_3–activated carbon composites for room temperature alcohol vapour detection. *Applied Physics A: Materials Science and Processing*, 128, pp.1–11. [https://doi.org/10.1007/s00339-022-05311-8]
14. Jerng, S.-K., Yu, D.S., Lee, J.H., Kim, C., Yoon, S. and Chun, S.-H., 2011. Graphitic carbon growth on crystalline and amorphous oxide substrates using molecular beam epitaxy. *Nanoscale Research Letters*, 6, 565. [https://doi.org/10.1186/1556-276X-6-565]
15. Kim, K.-H., Jahan, S.A. and Lee, J.-T., 2011. Exposure to formaldehyde and its potential human health hazards. *Journal of Environmental Science and Health, Part C*, 29(4), pp.277–299. [https://doi.org/10.1080/10590501.2011.629972]
16. Katsura, M., Nishimaki, K., Nakagawa, T., Yamamoto, T.A., Hirota, M. and Miyake, M., 1998. Thermodynamics of the formation of CH_4 by the reaction of carbon materials by a stream of NH_3. *Journal of Nuclear Materials*, 258-263, pp.839–842. [https://doi.org/10.1016/S0022-3115(98)00119-6]
17. Kumar, A. and Jena, H.M., 2016. Preparation and characterization of high surface area activated carbon from Fox nut (Euryale ferox) shell by chemical activation with H_3PO_4. *Results in Physics*, 6, pp.651–658. [https://doi.org/10.1016/j.rinp.2016.09.012]

18. Kyokunzire, P., Zaraket, J., Fierro, V. and Celzard, A., 2024. Recent developments in the use of activated carbon-based materials for gas sensing applications. *Journal of Environmental Chemical Engineering*, 12(5), p.113702. [https://doi.org/10.1016/j.jece.2024.113702]
19. Lennon, D., Lundie, D.T., Jackson, S.D., Kelly, G.J. and Parker, S.F., 2002. Characterization of activated carbon using X-ray photoelectron spectroscopy and inelastic neutron scattering spectroscopy. *Langmuir*, 18(12), pp.4667–4673. [https://doi.org/10.1021/la011749z]
20. Liu, Y., Liu, X., Dong, W., Zhang, L., Kong, Q. and Wang, W., 2017. Efficient adsorption of sulfamethazine onto modified activated carbon: A plausible adsorption mechanism. *Scientific Reports*, 7, pp.12437. [https://doi.org/10.1038/s41598-017-12805-6]
21. Luo, K.H., Yan, M., Hung, Y.H., Kuang, J.Y., Chang, H.C., Lai, Y.J. and Yeh, J.M., 2023. Polyaniline composites containing eco-friendly biomass carbon from agricultural waste coconut husk for enhancing gas sensor performance in hydrogen sulfide detection. *Polymers*, 15(23), pp.4554. [https://doi.org/10.3390/polym15234554]
22. Mochizuki, Y., Bud, J., Byambajav, E. and Tsubouchi, N., 2022. Influence of ammonia treatment on the CO_2 adsorption of activated carbon. *Journal of Environmental Chemical Engineering*, 10(2), p.107273. [https://doi.org/10.1016/j.jece.2022.107273]
23. Neme, I., Gonfa, G. and Masi, C., 2022. Activated carbon from biomass precursors using phosphoric acid: A review. *Heliyon*, 8(12), pp.e11940. [https://doi.org/10.1016/j.heliyon.2022.e11940]
24. Ogbodo, J.O., Arazu, A.V., Iguh, T.C., Onwodi, N.J. and Ezike, T.C., 2022. Volatile organic compounds: A proinflammatory activator in autoimmune diseases. *Frontiers in Immunology*, 13, pp.928379. [https://doi.org/10.3389/fimmu.2022.928379]
25. Ojha, R., Maniam, S., Rezaei Niya, S.M., Rigoni, A.S., Tran, K., Tanksale, A., Spencer, M.J.S. and Andrews, J., 2025. Insights into the structure-property relationships of activated carbon derived from phenolic resin for electrochemical storage of green hydrogen using proton battery. *Journal of Energy Storage*, 107, 114912. [https://doi.org/10.1016/j.est.2024.114912]
26. Prakash, J., Rao, P.T., Ghorui, S., Bahadur, J., Jain, V. and Dasgupt, K., 2022. Tailoring surface properties with O/N doping in CNT aerogel film to obtain sensitive and selective sensor for volatile organic compounds detection. *Sensors and Actuators B: Chemical*, 359, p.131606. [https://doi.org/10.1016/j.snb.2022.131606]
27. Qian, X., Li, N., Imerhasan, M. and Wang, W., 2019. Conversion of low molecular weight hydrogel to nitrogen-doped carbon materials and its application as supercapacitor. *Colloids and Surfaces A: Physicochemical and Engineering Aspects*, 573, pp.255–261. [https://doi.org/10.1016/j.colsurfa.2019.04.037]
28. Ranasinghe, R.A.S.R., Rathnathilaka, K.A.C., Karunarathna, P.G.D.C.K. and Samarasekar, P., 2024. Carbon gas sensors synthesized using Acacia auriculiformis tree branches to detect methanol, ethanol, acetone vapors and ammonia gas. *Ceylon Journal of Science*, 53(2), pp.207–218. [https://doi.org/10.4038/cjs.v53i2.8085]
29. Reinnig, M.C., Müller, L., Warnke, J. and Hoffmann, T., 2008. Characterization of selected organic compound classes in secondary organic aerosol from biogenic VOCs by HPLC/MS^n. *Analytical and Bioanalytical Chemistry*, 391(1), pp.171–182. [https://doi.org/10.1007/s00216-008-1990-y]
30. Rodiawan, S., Wang, S.-C. and Suhdi, 2024. Preparation and application of rubber fruit shell carbon as decoration material on ZnO for H_2S gas sensors. *Sensors and Materials*, 36(5), pp.1787. [https://doi.org/10.18494/sam4794]

31. Shen, Q., Liu, Y., Li, G. and An, T., 2024. A review of disrupted biological response associated with volatile organic compound exposure: Insight into identification of biomarkers. *Science of the Total Environment*, 948, pp.174924. [https://doi.org/10.1016/j.scitotenv.2022.174924]
32. Shimodaira, N. and Masui, A., 2002. Raman spectroscopic investigations of activated carbon materials. *Journal of Applied Physics*, 92, pp.902. [https://doi.org/10.1063/1.1487434]
33. Sun, Y., Zhang, G., Xu, Y. and Zhang, R., 2019. Catalytic performance of dioxide reforming of methane over Co/AC-N catalysts: Effect of nitrogen doping content and calcination temperature. *International Journal of Hydrogen Energy*, 44(31), pp.16424–16435. [https://doi.org/10.1016/j.ijhydene.2019.04.250]
34. Travlou, N.A., Seredych, M., Rodríguez-Castellon, E. and Bandosz, T.J., 2015. Activated carbon-based gas sensors: Effects of surface features on the sensing mechanism. *Journal of Materials Chemistry A*, 3(7), pp.3821–3831. [https://doi.org/10.1039/c4ta06161f]
35. Travlou, N.A., Ushay, C., Seredych, M., Rodríguez-Castellon, E. and Bandosz, T.J., 2016. Nitrogen-doped activated carbon-based ammonia sensors: Effect of specific surface functional groups on carbon electronic properties. *ACS Sensors*, 1(5), pp.591–599. [https://doi.org/10.1021/acssensors.6b00093]
36. Travlou, N.A. and Bandosz, T.J., 2017. Nanoporous carbon-composites as gas sensors: Importance of the specific adsorption forces for ammonia sensing mechanism. *Carbon*, 121, pp.114–126. [https://doi.org/10.1016/j.carbon.2017.05.048]
37. Ukanwa, K.S., Patchigolla, K., Sakrabani, R., Anthony, E. and Mandavgane, S., 2019. A review of chemicals to produce activated carbon from agricultural waste biomass. *Sustainability*, 11(22), pp.6204. [https://doi.org/10.3390/su11226204]
38. Xu, R.F., Mei, H., Chen, L., Tang, B., Lu, Q.Y., Cai, F.S., Yan, X., Zheng, J., Shen, X.T. and Yu, Y.J., 2023. Development and validation of an HPLC-MS/MS method for the simultaneous analysis of volatile organic compound metabolites, hydroxylated polycyclic aromatic hydrocarbons, and 8-hydroxy-2′-deoxyguanosine in human urine. *Journal of Chromatography B*, 1229, pp.123885. [https://doi.org/10.1016/j.jchromb.2023.123885]
39. Xue, C., Hao, W., Cheng, W., Ma, J. and Li, R., 2019. Effects of pore size distribution of activated carbon (AC) on CuCl dispersion and CO adsorption for CuCl/AC adsorbent. *Chemical Engineering Journal*, 375, pp.122049. [https://doi.org/10.1016/j.cej.2019.122049]
40. Zhang, L., Tu, L.-y., Liang, Y., Chen, Q., Li, Z.-s., Li, C.-h., Wang, Z.-h. and Li, W., 2018. Coconut-based activated carbon fibers for efficient adsorption of various organic dyes. *RSC Advances*, 8(74), pp.42280–42287. [https://doi.org/10.1039/c8ra08990f]